Chemosphere 168 (2017) 1389–1399

Contents lists available at ScienceDirect

Chemosphere

journal homepage: www.elsevier.com/locate/chemosphere

Contribution of petroleum-derived organic carbon to sedimentary organic carbon pool in the eastern Yellow Sea (the northwestern Pacific)

Jung-Hyun Kim [a, b, *], Dong-Hun Lee [a], Suk-Hee Yoon [a, 1], Kap-Sik Jeong [c], Bohyung Choi [a], Kyung-Hoon Shin [a, **]

[a] Department of Marine Science and Convergence Technology, Hanyang University ERICA Campus, 55 Hanyangdaehak-ro, Sangnok-gu, Ansan-si, Gyeonggi-do 426-791, South Korea
[b] Korea Polar Research Institute, 26 Songdomirae-ro, Yeonsu-gu, Incheon 21990, South Korea
[c] Marine Geology and Geophysics Division, Korea Institute of Ocean Science and Technology, Ansan 426-744, South Korea

HIGHLIGHTS

- The contribution of C_3 gymnosperms is the main source of *n*-alkanes in the eastern Yellow Sea.
- The contribution of petroleum-derived OC to the sedimentary OC pool is evident in the southern part of the study area.
- Our results indicate a possible influence of petroleum-induced OC on benthic food webs in this ecosystem.

ARTICLE INFO

Article history:
Received 28 June 2016
Received in revised form
19 November 2016
Accepted 20 November 2016
Available online 3 December 2016

Handling Editor: Shane Snyder

Keywords:
The Yellow Sea
n-alkanes
Petroleum
Carbon isotope
Gymnosperm

ABSTRACT

We investigated molecular distributions and stable carbon isotopic compositions ($\delta^{13}C$) of sedimentary *n*-alkanes (C_{15}–C_{35}) in the riverbank and marine surface sediments to trace natural and anthropogenic organic carbon (OC) sources in the eastern Yellow Sea which is a river dominated marginal sea. Molecular distributions of *n*-alkanes are overall dominated by odd-carbon-numbered high molecular weight *n*-C_{27}, *n*-C_{29}, and *n*-C_{31}. The $\delta^{13}C$ signatures of *n*-C_{27}, *n*-C_{29}, and *n*-C_{31} indicate a large contribution of C_3 gymnosperms as the main source of *n*-alkanes, with the values of −29.5 ± 1.3‰, −30.3 ± 2.0‰, and −30.0 ± 1.7‰, respectively. However, the contribution of thermally matured petroleum-derived OC to the sedimentary OC pool is also evident, especially in the southern part of the study area as shown by the low carbon preference index ($CPI_{25\text{-}33}$, <1) and natural *n*-alkanes ratio (NAR, <−0.6) values. Notably, the even-carbon-numbered long-chain *n*-C_{28} and *n*-C_{30} in this area have higher $\delta^{13}C$ values (−26.2 ± 1.5‰ and −26.5 ± 1.9‰, respectively) than the odd-carbon-numbered long-chain *n*-C_{29} and *n*-C_{31} (−28.4 ± 2.7‰ and −28.4 ± 2.4‰, respectively), confirming two different sources of long-chain *n*-alkanes. Hence, our results highlight a possible influence of petroleum-induced OC on benthic food webs in this ecosystem. However, the relative proportions of the natural and petroleum-derived OC sources are not calculated due to the lack of biogeochemical end-member data in the study area. Hence, more works are needed to constrain the end-member values of the organic material supplied from the rivers to the eastern Yellow Sea and thus to better understand the source and depositional process of sedimentary OC in the eastern Yellow Sea.

* Corresponding author. Korea Polar Research Institute, 26 Songdomirae-ro, Yeonsu-gu, Incheon 21990, South Korea.
** Corresponding author.
E-mail addresses: jhkim123@kopri.re.kr (J.-H. Kim), shinkh@hanyang.ac.kr (K.-H. Shin).
[1] Present address: Department of Fundamental Environment Research, Environmental Measurement & Analysis Center, National Institute of Environmental Research, Incheon 404-708, South Korea.

http://dx.doi.org/10.1016/j.chemosphere.2016.11.110
0045-6535/

1. Introduction

River-dominated marginal seas are one of the most important sites of organic carbon (OC) burial in the marine environment (e.g. Berner, 1982; Hedges et al., 1997). Hydrocarbons are ubiquitous in marine sediments and thus often used to decipher source information on allochthonous (terrestrial) and autochthonous (marine) OC in the marine environment (e.g. Prahl et al., 1994; Mead et al., 2005). Natural sources of hydrocarbons are terrestrial plants, aquatic (freshwater and marine) plants, and aquatic (freshwater and marine) algae and bacteria (e.g. Brassell et al., 1978). Terrestrial-derived hydrocarbons enter the marine environment by both atmospheric (winds, dust storms, forest fires and biomass burning) and aquatic (river discharges, continental run-offs) pathways (e.g. Simoneit et al., 1977). Hydrocarbons are also major components of petroleum, petroleum source rocks, and exposed continental rocks of intermediate thermal maturity (e.g. Brassell and Eglinton, 1980; Wang et al., 1999). These hydrocarbons can enter the marine environment through both natural (atmospheric and aquatic) inputs and anthropogenic processes (e.g. ship traffics, industrial activities). The petroleum-related hydrocarbon contamination in the marine environment has implications for the functioning of the benthic food web. For example, the unresolved complex mixture (UCM) of hydrocarbons, representing the majority of the petroleum hydrocarbons in marine sediments (e.g. Gough and Rowland, 1990), has been demonstrated to affect sediment-dwelling organisms (e.g. Smith et al., 2001; Scarlett et al., 2007). Hence, it is important to decouple the fractional contributions of petroleum-related hydrocarbons from other naturally occurring hydrocarbon sources in marine sediments.

The Yellow Sea (West Sea of Korea) is a semi-enclosed, northwestern Pacific marginal sea. Two of the largest rivers in the world, the Huanghe River (Yellow River) and the Changjiang River (Yangtze River) and several smaller Korean rivers (e.g. Han, Geum, and Youngsan Rivers) are flowing into the Yellow Sea, supplying high amounts of terrigenous sediments (e.g. Alexander et al., 1991; Yang et al., 2003; Yang and Youn, 2007). Accordingly, this marginal sea is considered to be an important sink for terrestrial OC (e.g. Chen and Borges, 2009). Previous studies on the origin and distribution of sedimentary OC in the Yellow Sea showed that the contribution of terrestrial OC was predominant along the coast while that of marine OC in the central basin (e.g. Xing et al., 2011, 2014). Some studies focused on hydrocarbons have indicated that terrestrial inputs are the major source of *n*-alkanes, mostly transported into the Yellow Sea by the Huanghe River discharge (e.g. Hu et al., 2009). However, most of the hydrocarbon-based studies have been focused on the western Yellow Sea, and comparable studies are rarely conducted in the eastern Yellow Sea. Hence, there is a tremendous lack of information regarding the eastern Yellow Sea.

In our previous study based on bulk (total organic carbon (TOC), C/N ratio, $\delta^{13}C_{TOC}$, and $\Delta^{14}C$) and molecular (glycerol dialkyl glycerol tetraethers) organic parameters (Yoon et al., 2016), we found that the sedimentary OC in the eastern Yellow Sea has a predominantly marine origin with a minor contribution of continental (i.e. soil- and lake/river-derived) OC. However, the $\Delta^{14}C$ values were depleted (on average $-227 \pm 53‰$, $n = 8$) suggesting that fossil OC, potentially derived from erosion of sedimentary bedrocks in the catchment areas and/or human activities such as waste discharges from rivers and oil spills due to shipping activities, is being contributed to the sedimentary OC pool in the eastern Yellow Sea. In this study, we examined sedimentary *n*-alkanes, by investigating their concentration, distribution, and $\delta^{13}C$ composition to evaluate the potential contribution of fossil (petroleum-derived) hydrocarbons to the sedimentary OC pool in the eastern Yellow Sea. For this purpose, we analysed 9 river bank sediments collected close to the river mouth of three major Korean rivers (Han, Geum, and Youngsan Rivers) and 66 surface sediments collected in the eastern Yellow Sea.

2. Material and methods

2.1. Riverbank and marine surface sediment sampling

Surface riverbank sediments (0–2 cm) were collected at 9 sites close to the river mouth of three major Korean rivers (Han, Geum, and Youngsan Rivers) flowing into the Yellow Sea (Fig. 1, see also Supplementary materials Appendix Table 1). Marine surface sediments (0–2 cm) were collected at 66 sites on the research vessel *R/V Eardo* of the Korea Institute of Ocean Science and Technology (KIOST) in 1998, 2000, 2001, and 2006 (Fig. 1, see also Supplementary materials Appendix Table 1). Note that a large amount of wastewater treatment sludge, sewage sludge, excretions, and organic wastewater was dumped into the area of ca. 3165 km^2 (38.0 km × 83.3 km) located 200 km off Gunsan city in the South Korea from 1988 to 2015 (Fig. 1). However, the sampling size within the dumping area ($n = 4$) was insufficient to handle the effect of the dumping activities in this study. A Van Veen grab sampler was deployed to collect samples. All samples were kept frozen at −20 °C prior to organic geochemical analysis.

2.2. Aliphatic hydrocarbon analysis

Sediments for the hydrocarbon analyses were freeze-dried and ground using a mortar and pestle. The homogenized riverbank samples were extracted with an Accelerated Solvent Extractor (ASE 200, Dionex) using a solvent mixture of dichloromethane/methanol (DCM/MeOH; 9/1 v/v) at 100 °C and a pressure of 1500 psi. Marine surface samples were ultrasonically extracted (3×) using a mixture of DCM/MeOH (9/1 v/v) for 20 min. The total lipid extracts were separated into three fractions on a silica gel column using hexane, hexane/DCM (1/1 v/v), and DCM/MeOH (1/1 v/v), respectively. The hexane (apolar) fractions were further purified over Ag+ impregnated silica pipette columns to separate saturated and unsaturated hydrocarbons using hexane as eluent.

The *n*-alkanes in selected saturated hydrocarbon fractions were identified with a Shimazu GC-2010 gas chromatograph interfaced to a Shimazu GCMS-QP2010 plus using a DB-5 fused silica capillary column (30 m × 0.25 mm i.d., the film thickness of 0.25 μm, J&W Scientific) with helium as a carrier gas. Mass scans were made in the range of m/z = 40–600 with 0.1 scan per second and an ionization energy of 70 eV. Samples were injected in the splitless mode. The temperature for both the injector and the detector was 310 °C. The oven program initiated at 70 °C and increased at a rate of 20 °C/min to 130 °C and subsequently by a rate of 4 °C/min until 320 °C. The final temperature of 320 °C was held for 25 min. Compound identifications were based on a comparison of relative GC retention times and mass spectra of the *n*-alkane mixture (C_8–C_{40}) analytical standards (Supelco 502065, AccuStandard, USA).

The saturated hydrocarbon fractions were further analysed for the quantification of *n*-alkanes on an Agilent Technologies 7890A gas chromatograph fitted with a fused-silica capillary column coated using a 30 m DB-5 column (0.25 mm i.d. and film thickness of 0.25 μm, J&W Scientific) and helium as a carrier gas. The oven program used was the same as for the GC/MS analysis. Quantification of chromatographically resolved aliphatic hydrocarbons was made by using external standards (solution of *n*-alkanes from *n*-C_8 to *n*-C_{40}, pristine, and phytane; Supelco 502065, AccuStandard,

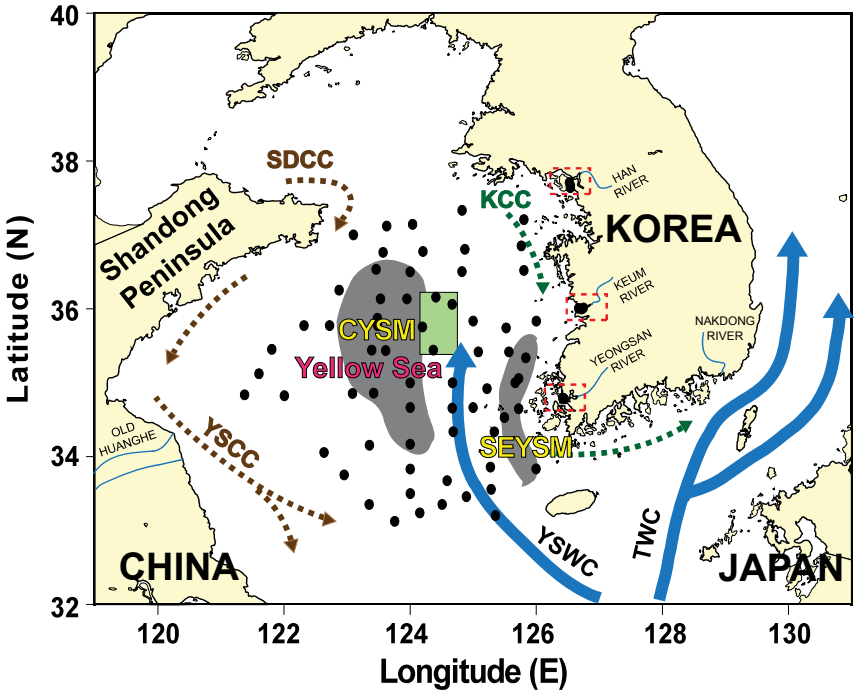

Fig. 1. (A) Schematic map showing the locations of riverbank and marine surface sediment samples with the surface circulation pattern and the muddy deposition areas in the Yellow Sea. SDCC = Shandong Coastal Current; YSCC = Yellow Sea Coastal Current; TWC = Tsushima Warm Current; YSWC = Yellow Sea Warm Current; KCC = Korea Coastal Current. The shaded areas represent the muddy deposition areas: the CYSM (Central Yellow Sea Mud) and the SEYSM (Southeastern Yellow Sea Mud). The filled rectangle (green) indicates the dumping area. (For interpretation of the references to colour in this figure legend, the reader is referred to the web version of this article.)

USA). The UCM is calculated using the mean response factors of *n*-alkanes. Data were acquired and integrated using the Chemstation chromatography manager software.

The average chain length (ACL; Cranwell et al., 1987; Poynter and Eglinton, 1990), the carbon preference index (CPI, Bray and Evans 1961), the terrestrial/aquatic ratio (TAR; odd-carbon-numbered long-chain/odd-carbon-numbered short-chain alkanes; Bourbonnière and Meyers, 1996), the Pmar-aq (% of aquatic plants, Ficken et al., 2000; Mead et al., 2005), and the natural *n*-alkanes ratio (NAR; Mille et al., 2007) of *n*-alkanes were calculated as follows:

$$\mathrm{ACL} = \frac{[25\times C25 + 27\times C27 + 29\times C29 + 31\times C31 + 33\times C33]}{[C25 + C27 + C29 + C31 + C33]} \quad (1)$$

$$\mathrm{CPI} = \frac{1}{2}\times\left[\left(\frac{C25 + C27 + C29 + C31 + C33}{C24 + C26 + C28 + C30 + C32}\right) + \left(\frac{C25 + C27 + C29 + C31 + C33}{C26 + C28 + C30 + C32 + C34}\right)\right] \quad (2)$$

$$\mathrm{TAR} = \frac{[C27 + C29 + C31]}{[C15 + C17 + C19]} \quad (3)$$

$$\mathrm{Pmar-aq} = \frac{[C23 + C25]}{[C23 + C25 + C29 + C31]} \quad (4)$$

$$\mathrm{NAR} = \frac{[\sum C19 - 32] - [2\times(\sum \mathrm{even}\ C20 - 32)]}{[\sum C19 - 32]} \quad (5)$$

where Ci is the concentration of the *n*-alkane containing i carbon atoms.

2.3. Compound-specific stable carbon isotope analyses

With the same apolar fractions, the stable carbon isotope ($\delta^{13}C$) composition of *n*-alkanes was determined using a gas chromatography-combustion-isotope ratio mass spectrometry (GC-C-IRMS). A combustion interface (packed with copper oxide, operated at 850 °C) of the isotope ratio mass spectrometer (Isoprime, GV Instruments) was connected with a gas chromatograph (Hewlett Packard 6890 N; Agilent Technology). The samples were subjected to the same temperature conditions and capillary column described for the GC/MS analysis. Calibration was performed by injecting several pulses of reference gas CO_2 of known $\delta^{13}C$ value at the beginning and the end of each GC run. $\delta^{13}C$ values were further calibrated using a certified isotope standard (Alkane mixture type A6, Indiana University, USA). This standard was repeatedly analysed every 5 sample runs. The correlation coefficients (r^2) of the known $\delta^{13}C$ values of the *n*-alkane isotope standard (C_{16} to C_{30}) with the average values of the measured ones were higher than 0.99. The analytical precision was better than ±0.6‰, as determined by repeated injections of the standard. Isotopic ratios are expressed as $\delta^{13}C$ values in per mil relative to the Vienna-PeeDee Belemnite (VPDB).

2.4. Statistical analyses

Fractional abundances of *n*-alkane compounds (C_{15}–C_{35}) were obtained by normalizing each concentration to the summed concentration of all *n*-alkane homologues considered. Principal Component Analysis (PCA) was performed on the fractional abundance data of *n*-alkane to provide a general view of the variability of the distribution of *n*-alkane by using the R program (R-Development-Core-Team, 2015).

3. Results

3.1. Riverbank sediments

The GC-FID chromatograms of the riverbank sediment samples showed fairly uniform patterns with a broad UCM and a series of resolved compounds (Fig. 2A). The UCM concentrations as a proportion of TOC in the sediment ranged from 36 to 422 μg/g TOC (average: 134 ± 112 μg/g TOC, $n = 9$; Fig. 3A). The resolved *n*-alkanes superimposed on a broad UCM ranged from *n*-C_{15} to *n*-C_{35} in all investigated riverbank sediments with the concentrations of 167–1334 μg/g TOC (average: 763 ± 333 μg/g TOC, $n = 9$; Supplementary materials Appendix Table 2). The summed concentrations of odd-carbon-numbered long-chain *n*-alkanes (C_{25} to

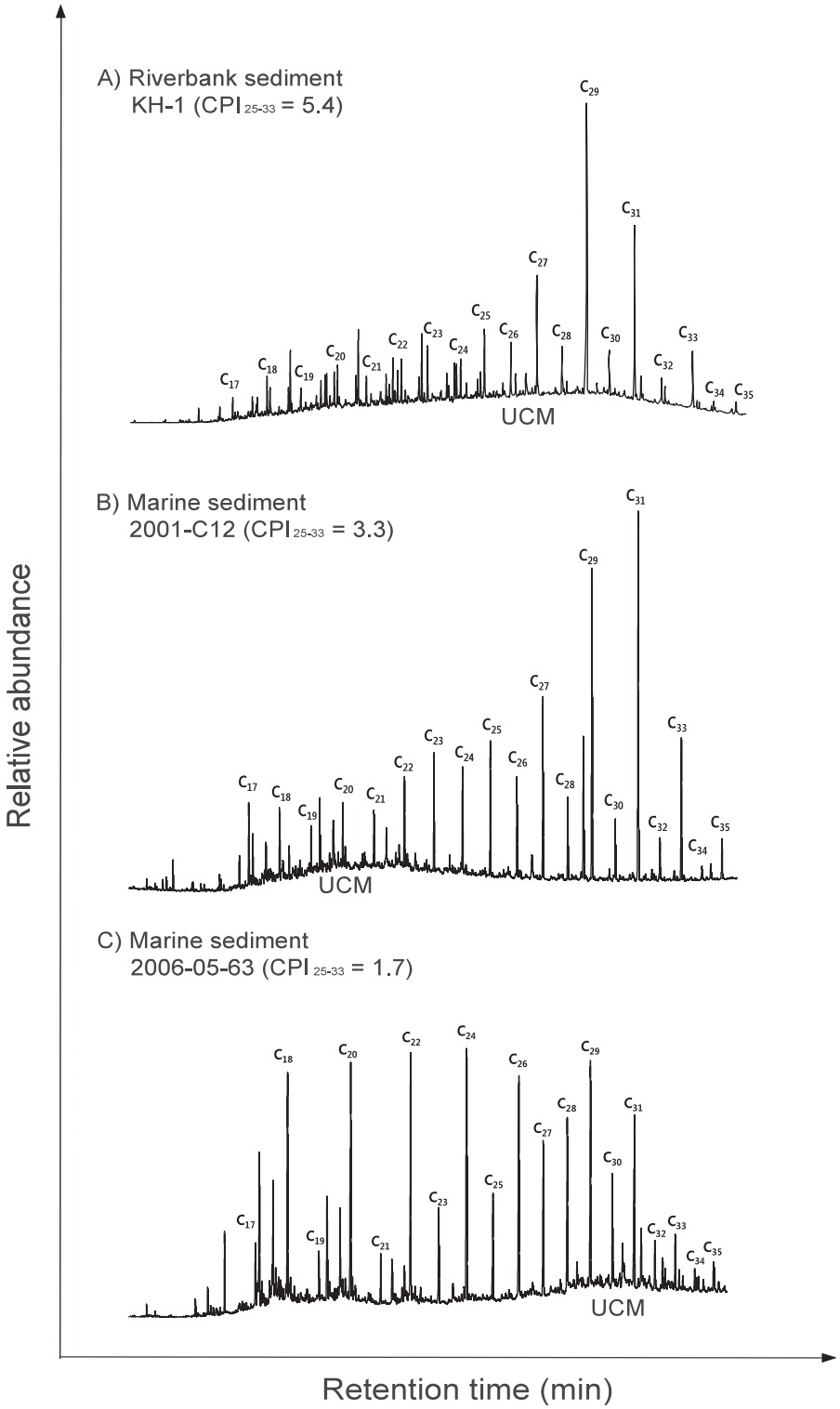

Fig. 2. Examples of GC-FID chromatograms of *n*-alkanes in riverbank and marine surface sediments: (A) riverbank sediment (KH-1), (B) marine surface sediment (2001-C12), and (C) marine surface sediment (2006-05-63). C*x* refers to *n*-alkane (*n*-C*x*) peaks, where "*x*" is a number of carbon atoms.

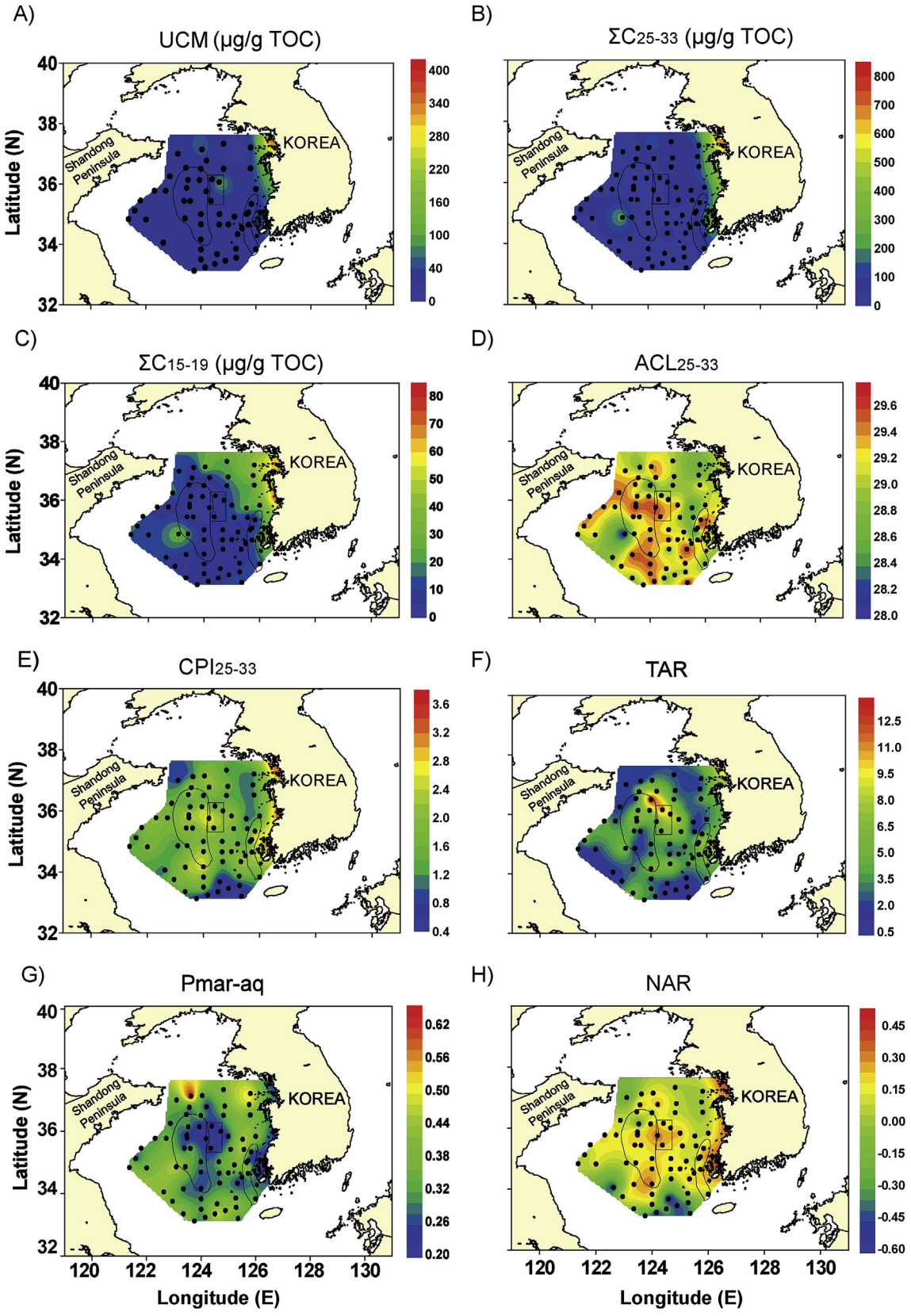

Fig. 3. Spatial distributions of various *n*-alkane parameters: concentrations of (A) unresolved complex mix (UCM), (B) odd-carbon-numbered long-chain *n*-alkanes (C_{25}–C_{35}) and (C) odd-carbon-numbered short-chain *n*-alkane (C_{15}–C_{19}), (D) average chain length (ACL_{25-35}), (E) carbon preference index (CPI_{25-35}), (F) terrestrial/aquatic ratio (TAR), (G) % of aquatic plants (Pmar-aq), and (H) natural *n*-alkanes ratio (NAR).

C_{33}; ΣC_{25-33}) normalized to TOC ranged from 75 to 787 μg/g TOC (average: 414 ± 200 μg/g TOC, $n = 9$; Fig. 3B), while those of odd-carbon-numbered short-chain *n*-alkanes (C_{15} to C_{19}; ΣC_{15-19}) varied between 17 and 79 μg/g TOC (average: 49 ± 20 μg/g TOC, $n = 9$; Fig. 3C). *n*-C_{29} was the major *n*-alkane in the riverbank sediments (Fig. 2A), with the ACL_{25-33} values of 29.1 ± 0.1 (Fig. 3D). The *n*-alkanes exhibit an odd-carbon-number predominance with CPI_{25-33} values varying between 2.5 and 3.6 (Fig. 3E). The TAR, the Pmar-aq, and the NAR ranged from 4 to 10, from 0.2 to 0.3, and from 0.3 to 0.5, respectively (Fig. 3F–H). Three selected samples were analysed for the carbon stable isotope compositions of *n*-alkanes. The *n*-alkenes with sufficient concentrations for the isotope measurements ranged from *n*-C_{17} to *n*-C_{31}. The $\delta^{13}C$ data of *n*-alkanes showed that odd-carbon-numbered *n*-alkanes (C_{17}–C_{31}) ranged from −32.7‰ to −22.4‰, whereas the even-carbon-numbered *n*-alkanes (C_{18}–C_{30}) varied between −31.7‰ and −25.2‰ (Supplementary materials Appendix Table 3).

3.2. Marine surface sediments

The GC-FID chromatograms of the marine surface sediments showed non-uniform patterns with a UCM and a series of resolved compounds (Fig. 2B–C). The UCM concentrations varied between 1 and 105 μg/g TOC (average: 10 ± 19 μg/g TOC, $n = 66$; Fig. 3A). A homologous series of *n*-alkanes from *n*-C_{15} to *n*-C_{35} was also detected in all marine surface sediments (Fig. 2B–C). Total resolved *n*-alkane concentrations ranged from 21 to 607 μg/g TOC (average: 130 ± 109 μg/g TOC, $n = 66$; Supplementary materials Appendix Table 2). The ΣC_{25-33} varied between 6 and 251 μg/g TOC (average: 48 ± 40 μg/g TOC, $n = 66$; Fig. 3B). The ΣC_{15-19} ranged from 2 to 44 μg/g TOC (average: 11 ± 9 μg/g TOC, $n = 66$; Fig. 3C). In general, *n*-alkane distributions in marine sediments were characterized by a peak at *n*-C_{29} or *n*-C_{31} (Fig. 2B–C). The ACL_{25-33} showed quite stable values between 28.0 and 29.7 (Fig. 3D) while the CPI_{25-33} values varied between 0.4 and 2.9 (Fig. 3E). The TAR, the Pmar-aq, and the NAR ranged from 1 to 9, from 0.2 to 0.5, and from −0.6 to 0.4, respectively (Fig. 3F–H). Twenty-six selected samples were analysed for the carbon stable isotope compositions of *n*-alkanes. Similar to the riverbank sediments, the *n*-alkenes with sufficient concentrations for the isotope measurements ranged from *n*-C_{17} to *n*-C_{31}. The $\delta^{13}C$ data of *n*-alkanes showed that odd-carbon-numbered *n*-alkanes (C_{17}–C_{31}) ranged from −35.6‰ to −23.6‰, whereas the even-carbon-numbered *n*-alkanes (C_{18}–C_{30}) varied between −33.1‰ and −24.1‰ (Supplementary materials Appendix Table 3).

3.3. Statistical analyses

Principal component analysis (PCA) was performed on the fractional abundance data to examine a general variability of the distribution of *n*-alkanes (C_{15} to C_{35}). For all surface sediments investigated, the first two principal components explained a cumulative 56.4% of the variance (Fig. 4A). On the first principal component (PC1, explaining 33.5% of the variance) the loading of odd-carbon-numbered long-chain *n*-alkanes (C_{25} to C_{35}) was opposite to that of all even-carbon-numbered long-chain *n*-alkanes (C_{16} to C_{34}). On the second principal component (PC2, explaining 22.9% of the variance), odd- and even-carbon-numbered short-chain *n*-alkanes (C_{15} to C_{23}) were positively loaded while odd- and even-carbon-numbered long-chain *n*-alkanes (C_{24} to C_{35}) were negatively loaded. We also performed a hierarchical clustering of principal components (HCPC) on the PCA results to cluster samples with similar brGDGT distributions. The samples investigated were grouped into four distinct clusters, i.e. Cluster1, Cluster2, Cluster3 and Cluster4 (Fig. 4B). The averaged molecular distribution of *n*-alkanes in each cluster was shown in Fig. 4C–F.

4. Discussion

4.1. Concentration and molecular distribution of sedimentary *n*-alkanes

Natural sources of straight chain alkanes (*n*-alkanes) in the marine environment are complex and of diverse origins: terrestrial plants, aquatic (freshwater and marine) plants, and aquatic (freshwater and marine) algae and bacteria. The odd-carbon-numbered high molecular weight *n*-alkanes (>C_{25}) indicate a mainly terrestrial vascular plant input, maximizing at *n*-C_{27}, *n*-C_{29}, and *n*-C_{31} (e.g. Eglinton and Hamilton, 1967; Tissot et al., 1977), while the odd-carbon-numbered short chain *n*-alkanes (C_{15} to C_{19}) are typical of aquatic algal and photosynthetic bacterial input, maximizing at *n*-C_{17} (e.g. Han and Calvin, 1969; Meyers and Ishlwatari, 1993). Moreover, the odd-carbon-numbered mid-molecular weight *n*-alkanes are an origin of freshwater and marine non-emergent (submerged and floating) macrophytes with the maximum at *n*-C_{21}, *n*-C_{23}, and *n*-C_{25} (e.g. Huang et al., 1999; Ficken et al., 2000; Mead et al., 2005). The *n*-alkane distributions of freshwater emergent plants are between freshwater non-emergent and terrestrial plants. The *n*-alkane maxima at *n*-C_{29} and *n*-C_{31} (Fig. 2) with the ACL_{25-33} of ~29 (Fig. 3D) in riverbank and marine sediments are thus evidence for an origin of predominantly epicuticular leaf waxes of higher land plants. Some studies have shown that the *n*-alkane distributions of C_3 grasses are generally dominated by *n*-C_{31}, whereas those of C_3 trees and shrubs tend to show large proportions of *n*-C_{27} and *n*-C_{29} (e.g. Cranwell, 1973; Meyers and Ishlwatari, 1993; Meyers, 2003; Bi et al., 2005; Rommerskirchen et al., 2006). Hence, a shift in the carbon number maximum from *n*-C_{27} to *n*-C_{31} with higher ACL_{25-33} values and *n*-C_{27}/*n*-C_{31} ratios of <1 might hint an increased contribution of C_3 grasses relative to trees and shrubs to marine sediments. The ACL_{25-33} values are generally higher in offshore sites (Fig. 3D) with *n*-C_{27}/*n*-C_{31} ratios of <1 (Supplementary materials Appendix Table 2), implying an increasing contribution of *n*-alkanes derived from C_3 grasses to marine sediments.

In general, short-chain *n*-alkanes homologues are dominated by *n*-C_{17} in the riverbank and marine sediments (Fig. 1), indicative of algal and photosynthetic bacterial contributions (e.g. Han and Calvin, 1969). However, some marine sediments exhibit even carbon-number preference in the range of *n*-C_{16} to *n*-C_{22} (Supplementary materials Appendix Table 2) which can be ascribed to non-photosynthetic bacterial sources (Han et al., 1968; Grimalt and Albaiges, 1987). Since *n*-C_{29} and *n*-C_{31} are abundant in higher land plants and *n*-C_{17} is prominent in aquatic organisms, *n*-C_{17}/*n*-C_{29} or *n*-C_{17}/*n*-C_{31} ratios reflect the relative contributions of autochthonous (>1) and allochthonous (<1) *n*-alkanes to marine sediments (Supplementary materials Appendix Table 2). Most of riverbank and marine sediments have lower values of these radios (i.e. <1), suggesting that sedimentary *n*-alkanes are mostly of allochthonous, terrestrial origin. This is in good agreement with the results that the concentration of ΣC_{25-33} is one order higher than that of ΣC_{15-19} (Fig. 3B and C). The TAR (odd-carbon-numbered long-chain/odd-carbon-numbered short-chain alkanes; Bourbonnière and Meyers, 1996) values are also high, especially along the coast and in the CYSM (Central Yellow Sea Mud) and SEYSM (Southeastern Yellow Sea Mud) deposits (Fig. 3F), indicative of higher terrestrial sources of *n*-alkanes relative to marine sources. Furthermore, the Pmar–aq can be applied to distinguish between terrestrial plants and aquatic plants with mid-length *n*-alkanes (Ficken et al., 2000; Mead et al., 2005). Low values (0.01–0.3) of the

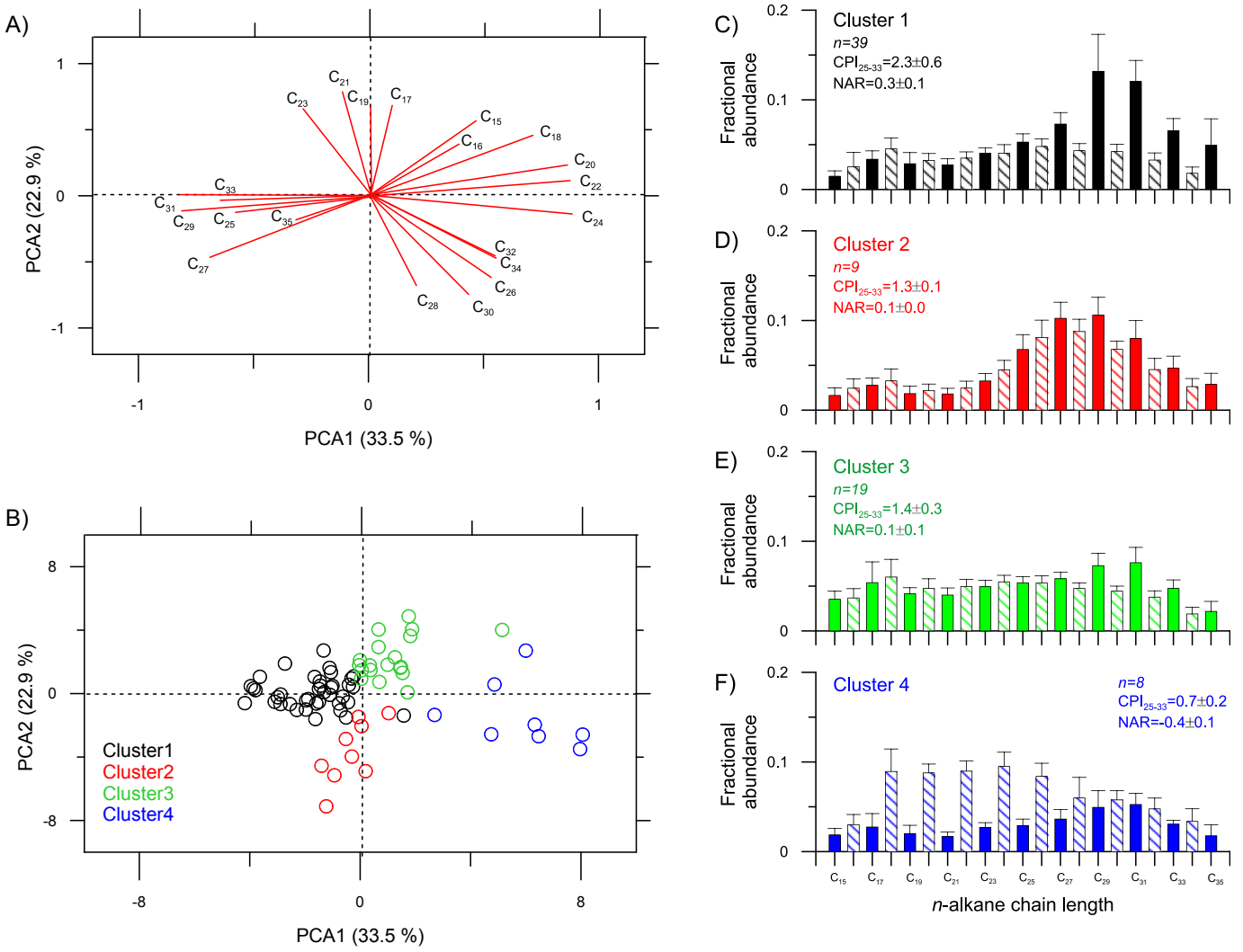

Fig. 4. Results of (A) the Principal Component Analysis (PCA) and (B) the Hierarchical Clustering on Principal Components (HCPC) of the fractional abundances of *n*-alkanes, and (C–F) the average *n*-alkane distributions of the corresponding clusters.

Pmar–aq correspond to terrestrial plants, mid-values (~0.4–0.6) to aquatic (freshwater and marine) emergent macrophytes including mangroves, and high values (>0.6) to aquatic (freshwater and marine) non-emergent macrophytes in coastal marine environments (e.g. Ficken et al., 2000; Sikes et al., 2009). Thus, low Pmar–aq values in the riverbank sediments and in the CYSM (Central Yellow Sea Mud) deposit reflect predominant contributions of terrestrial higher plants to the sediments (Fig. 3G). The sedimentary *n*-alkanes in other offshore sites might be a mixture of marine non-emergent macrophytes such as seagrasses with terrestrial higher vascular plants as indicated by high Pmar–aq values, given that mangroves do not occur in the study area (Fig. 3G).

The UCM contains a large number of structurally complex isomers, most of which are homologues of linear, branched and/or cyclic alkanes (e.g. Gough and Rowland, 1990). Usually, the ratio of the UCM to resolved components (U/R) > 4 can be a sign of a substantial petroleum input (Mazurek and Simoneit, 1984). In our samples, the U/R ratio was generally less than 1, suggesting a minor input of petroleum to the riverbank and marine sediments investigated in this study. However, it is worth to note that the UCM concentrations were higher near the river mouth and in the dumping area (Fig. 3A). This might be indicative of the waste discharges from rivers and the waste dumping activities in the western Yellow Sea. The CPI of sedimentary *n*-alkanes can be another measure of petroleum inputs. Epicuticular waxes derived from higher plants generally have high CPI (>4) values (e.g. Eglinton and Hamilton, 1963; Mazurek and Simoneit, 1984), while petroleum-derived *n*-alkanes have a CPI of 1 (e.g. Simoneit, 1984). The average CPI_{25-33} value of the riverbank sediments is 3.2 ± 0.3 (Supplementary materials Appendix Table 2), thus typical of terrestrial sources, i.e. land-plant epicuticular waxes. However, the samples from the southern part of the study area have the CPI_{25-33} values as low as 0.4 (Fig. 3E). This suggests that petroleum-derived *n*-alkanes contribute to sedimentary *n*-alkanes in that area. Furthermore, the NAR (Mille et al., 2007) roughly estimate the proportions of natural and petroleum *n*-alkanes. This ratio is close to or below zero for petroleum hydrocarbons and close to one for higher terrestrial plants or aquatic plants. Consistent to the results from the CPI_{25-33}, the NAR values from the southern part of the study area are as low as −0.6, while the average value of the riverbank sediments is 0.4 ± 0.0 (Fig. 3H). The ratio of *n*-C_{18} over *n*-C_{17} close to one might also be indicative of dominant input of petroleum-derived *n*-alkanes compared to natural inputs (Jeng and Huh, 2004). The values of *n*-C_{18}/*n*-C_{17} in the riverbank and marine sediments are mostly higher than 1 (Supplementary materials

Appendix Table 2), indicating that petroleum-derived *n*-alkanes are being deposited in the eastern Yellow Sea.

Alternatively, the presence of the UCM in the aliphatic fraction might be linked to bacterial degradation of natural organic compounds such as algal detritus (e.g. Gough and Rowland, 1990). Photosynthetic algae and bacteria might contain *n*-C_{17} as the most abundant hydrocarbon component while non-photosynthetic bacteria have hydrocarbon distributions dominated by other *n*-alkanes such as *n*-C_{18} (e.g. Han et al., 1968; Han and Calvin, 1969). Consequently, higher values of *n*-C_{18} over *n*-C_{17} (i.e. >1) in our samples might be attributed to a higher contribution of non-photosynthetic bacteria rather than that of photosynthetic algae and bacteria (Jeng and Huh, 2004). Notably, the spatial distribution patterns of the UCM (Fig. 3A) and the *n*-C_{18}/*n*-C_{17} ratio (data not shown) are different in comparison to those of the CPI_{25-33} (Fig. 3E) and the NAR (Fig. 3H). This difference provides a hint that at least, parts of the UCM and short-chain *n*-alkanes in the range of *n*-C_{16} to *n*-C_{22} might be derived from bacterial degradation of natural organic inputs.

The PCA results show that the PC1 (33.5%) is closely related to odd-carbon-numbered long-chain *n*-alkanes (C_{25} to C_{35}) with a negative loading and a positive loading of all even-carbon-numbered *n*-alkanes (C_{16} to C_{34}) (Fig. 4A). The PC2 (22.9%) predominantly reflects the presence of short- and medium-chain *n*-alkanes (C_{15} to C_{23}) with a positive loading and the long-chain *n*-alkanes (C_{25} to C_{35}) with a negative loading (Fig. 4A). The subsequent HCPC results show that the riverbank sediments belong to Cluster 1 which is associated with odd-carbon-numbered long-chain *n*-alkanes (Fig. 4B). In contrast, the marine surface sediments are subgrouped in Cluster 1 to Cluster 4 (Fig. 4B). Cluster 4 is closely linked to even-carbon-numbered *n*-alkanes, while Cluster 3 is more associated with short-to medium-chain *n*-alkanes (Fig. 4B). Cluster 4 has the lowest average CPI_{25-33} value of 0.7 (Fig. 4F), while that of Cluster 1 is the highest one of 2.3 (Fig. 4C). Furthermore, Cluster 4 has the average NAR value of −0.4, while that of Cluster 1 is 0.3. Cluster 2 and Cluster 3 show intermediate CPI_{25-33} (1.3 and 1.4, respectively) and NAR (0.1 and 0.1, respectively) values between Cluster 1 and Cluster 4 (Fig. 4D and E). Notably, most of the samples belonging to Cluster 4 are located in the southern part of the study area (Fig. 5), where the CPI_{25-33} (Fig. 3E) and the NAR (Fig. 3H) are as low as 0.4 and −0.6, respectively. Hence, it appears that Cluster 1 is represented by the dominance of terrestrial sources of *n*-alkanes, i.e. land-plant epicuticular waxes. In contrast, Cluster 4 displays a dominance of the petroleum-derived *n*-alkanes, probably with an additional contribution of non-photosynthetic bacterial sources as indicated by the even carbon-number preference in the short-chain *n*-alkanes. Cluster 2 and Cluster 3 contain a slightly different degree of a mixed terrestrial and petroleum sources of *n*-alkanes. Considering that Cluster 3 has a higher proportion of odd-carbon-numbered short-to medium-chain *n*-alkanes (C_{17} to C_{23}) than Cluster 2 (Fig. 4D and E), the contribution of aquatic sources of *n*-alkanes such as algae and photosynthetic bacteria and/or non-emergent macrophytes to sedimentary *n*-alkanes might be higher in Cluster 3 than in Cluster 2.

4.2. Molecular isotopic composition of sedimentary n-alkanes

The stable isotopic compositions of the solvent extractable *n*-alkanes are grouped for each cluster and the average values of individual *n*-alkanes are shown in Fig. 6. The carbon isotopic signatures of a biomarker are a useful mean to distinguish among

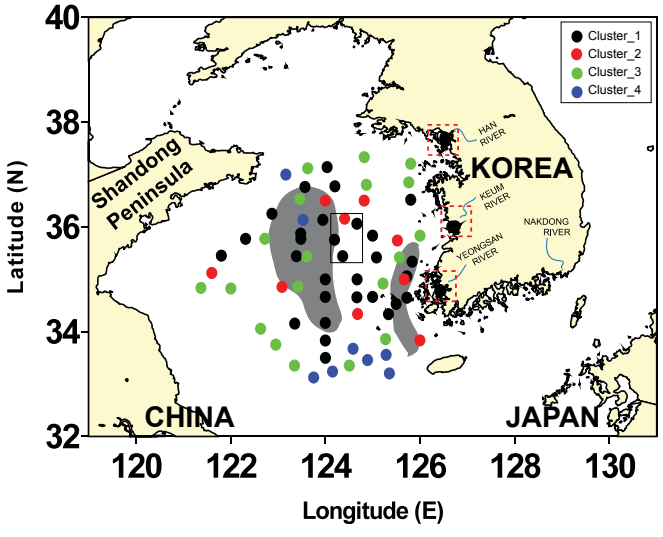

Fig. 5. Spatial distribution patterns of 4 clusters obtained from the HCPC (see also Fig. 4).

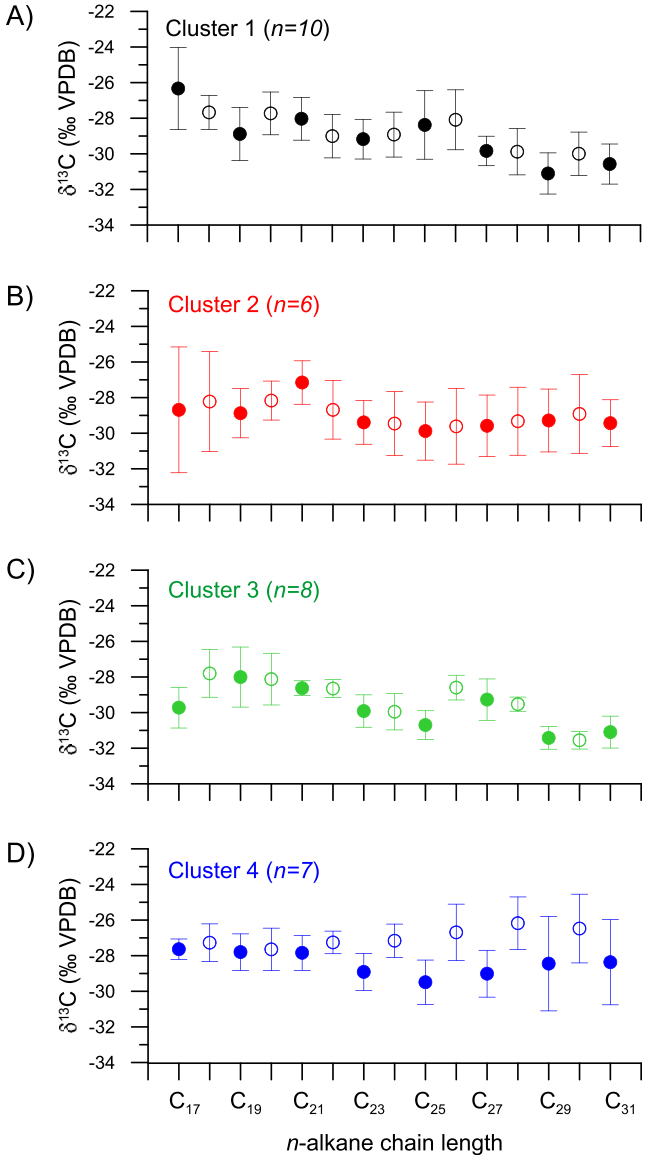

Fig. 6. Average $\delta^{13}C$ values of each cluster ranging from *n*-C_{17} to *n*-C_{31}: (A) Cluster 1, (B) Cluster 2, (C) Cluster 3, and (D) Cluster 4.

sources (e.g. Freeman et al., 1990; Collister et al., 1992). Specific lipids are typically depleted in ^{13}C content with respect to the corresponding bulk tissue as a consequence of biosynthetic fractions and related effects (e.g. Hayes, 1993), with an offset ($\delta^{13}C_{bulk}$–$\delta^{13}C_{biomarker}$) of 5–10‰ for algae and 7–10‰ for vascular plants (e.g. Collister et al., 1994; Ballentine et al., 1996; Schouten et al., 1998; Wiesenberg et al., 2004). The *n*-alkane $\delta^{13}C$ values of terrestrial C_3 plants range from −39‰ to −33‰, generally ~8‰ lighter than those of bulk tissues (e.g. Bird et al., 1995; Collister et al., 1994; Chikaraishi and Naraoka, 2003). Furthermore, $\delta^{13}C$ values are lower in C_3 angiosperms (−33.9 ± 3.2‰) than in C_3 gymnosperms (−30.0 ± 1.5‰) for odd-carbon-numbered long-chain *n*-alkanes from C_{27} to C_{31} (Chikaraishi and Naraoka, 2003; Pedentchouk et al., 2008), reflecting a difference in plant physiology such as stomatal conductance for CO_2 and H_2O vapour between two species (Pedentchouk et al., 2008). The $\delta^{13}C$ signatures of *n*-C_{27}, *n*-C_{29}, and *n*-C_{31} are within a relatively narrow range for each cluster and centered at −29.5 ± 1.3‰, −30.3 ± 2.0‰, and −30.0 ± 1.7‰, respectively (Fig. 6). Hence, the $\delta^{13}C$ signatures of all four clusters fell in the range expected for C_3 gymnosperms leaf waxes (Chikaraishi and Naraoka, 2003; Pedentchouk et al., 2008). This indicates that the long-chain *n*-alkane contribution of C_3 gymnosperms to the sedimentary *n*-alkanes is much greater than that of C_3 angiosperms in the eastern Yellow Sea.

Freshwater non-emergent (submerged and floating) macrophytes are characterized by an abundance maximum at *n*-C_{21}, *n*-C_{23} or *n*-C_{25} (e.g. Barnes and Barnes, 1978; Cranwell, 1984; Ogura et al., 1990; Viso et al., 1993; Baas et al., 2000; Ficken et al., 2000), with the $\delta^{13}C$ values of −24.0 ± 0.3‰, −24.9 ± 1.5‰, and −25.4 ± 1.8‰, respectively (Chikaraishi and Naraoka, 2003). Alternatively, the *n*-alkanes of C_{21} to C_{25} can be also an origin of marine non-emergent macrophytes (i.e. seagrasses), with enriched isotopic signals of approximately −13 to −22‰ (e.g. Canuel and Martens, 1993; Canuel et al., 1997; Ficken et al., 2000; Jaffé et al., 2001; Mead et al., 2005). The average $\delta^{13}C$ values of *n*-C_{21}, *n*-C_{23} and *n*-C_{25} are −27.9 ± 1.2‰, −29.3 ± 1.1‰, and −29.3 ± 1.8‰, respectively, with relatively small differences between the clusters (Fig. 6). Thus, the depleted isotope values of the odd-carbon-numbered mid-chain *n*-alkanes suggest a negligible contribution of freshwater and marine non-emergent macrophytes to marine sediments.

The $\delta^{13}C$ values of *n*-C_{17} from the investigated sediments varies between −35.6 and −22.4‰, with the average values of −26.3 ± 2.3‰ and −28.7 ± 2.2‰ for Cluster 1 and for Cluster 2 to Cluster 4, respectively (Fig. 6). Depleted $\delta^{13}C$ values of *n*-C_{17} (−36 to −34‰) were reported for cyanobacteria (van der Meer et al., 2000; Kristen et al., 2010). In contrast, heavier $\delta^{13}C$ values of *n*-C_{17} (−24 to −23‰) were shown for freshwater non-emergent plants (Chikaraishi and Naraoka, 2003). The short-chain *n*-alkane, *n*-C_{17} is produced not only by algae and photosynthetic bacteria (Han and Calvin, 1969) but also by non-photosynthetic bacteria and other heterotrophs, such as ciliated protozoa (Han and Calvin, 1969; Cranwell et al., 1987). Hence, the large variability of $\delta^{13}C$ values of *n*-C_{17} observed in the marine sediments might be related to multiple sources of *n*-C_{17}, possibly with different metabolic pathways (e.g., photoautotrophs and heterotrophs; Garcin et al., 2012).

In terrestrial plants, odd-carbon-numbered long-chain *n*-alkanes are in general enriched in ^{13}C relative to even-carbon-numbered long-chain *n*-alkanes (Chikaraishi and Naraoka, 2003). However, in our dataset, even-carbon-numbered long-chain *n*-alkanes (C_{28} to C_{30}) have higher $\delta^{13}C$ values than corresponding odd-carbon-numbered long-chain *n*-alkanes (C_{29} to C_{31}) (Fig. 6). Moreover, the range of $\delta^{13}C$ values is much larger in even-carbon-numbered long-chain *n*-alkanes than in odd-carbon-numbered long-chain *n*-alkanes (Fig. 6). This indicates that there are probably different sources of even-carbon-numbered long-chain *n*-alkanes in addition to terrestrial C_3 plants. It is worthwhile to note that Cluster 4 shows a distinct zigzag pattern in $\delta^{13}C$, with the strongly enriched $\delta^{13}C$ values of even-carbon-numbered long-chain *n*-alkanes in comparison to those of Cluster 1 to Cluster 3 (Fig. 6). Recently, Tao et al. (2015) investigated suspended particulate matter (SPM) collected at Kenli, ~50 km upstream of the Yellow River, which accounts for roughly 89% of sediment flux to the adjacent Bohai Sea and the Yellow Sea (Milliman and Syvitski, 1992). The authors observed that the abundance-weighted average $\delta^{13}C$ values of *n*-C_{29+31} in SPM (−30.3 ± 1.1‰, $n = 7$) was depleted in comparison to those of *n*-$C_{26+28+30+32}$ (−29.1 ± 1.0‰, $n = 7$). Notably, the abundance-weighted average $\Delta^{14}C$ value of *n*-C_{29+31} was higher (−480 ± 121‰) than that of *n*-$C_{26+28+30+32}$ (−867 ± 112‰). Accordingly, the ^{14}C age of *n*-C_{29+31} was younger (5379 ± 1829) than that of *n*-$C_{26+28+30+32}$ (18,711 ± 7066). The older ^{14}C ages of *n*-$C_{26+28+30+32}$ imply a higher *n*-alkane input of fossil (i.e. petrogenic/anthropogenic) origin in the Yellow River drainage basin (Tao et al., 2015). Similarly, it seems likely that the enriched $\delta^{13}C$ values of the even-carbon-numbered long-chain *n*-alkanes (C_{28} to C_{30}) in our data set are owing to fossil-derived *n*-alkanes inputs.

5. Conclusions

Molecular distributions of *n*-alkanes together with their stable carbon isotopic compositions are applied to riverbank sediments collected from three major Korean rivers (Han, Geum, and Youngsan Rivers) flowing into the Yellow Sea as well as marine surface sediments collected in the eastern Yellow Sea. Based on the molecular distributions (C_{15} to C_{35}), *n*-alkanes are largely suggested to originate from C_3 tree leaves, indicated by the dominance of *n*-C_{27}, *n*-C_{29}, and *n*-C_{31}. The average $\delta^{13}C$ values of *n*-C_{27} (−29.5 ± 1.3‰), *n*-C_{29} (−30.3 ± 2.0‰), and *n*-C_{31} (−30.0 ± 1.7‰) suggest a greater contribution of C_3 gymnosperms as a source of *n*-alkanes in the eastern Yellow Sea. The PCA and subsequent HCPC analyses of the fractional abundances of *n*-alkanes result in four distinct clusters, highlighting the heterogenous sources of sedimentary *n*-alkanes in the western Yellow Sea. Especially, the marine surface sediments from the southern part of the study area (Cluster 4) are subgrouped with the low $CPI_{25\text{-}33}$, (<1) and NAR (<−0.6) values. Notably, *n*-C_{28} and *n*-C_{30} in this area have much higher $\delta^{13}C$ values (−26.2 ± 1.5‰ and −26.5 ± 1.9‰, respectively) than *n*-C_{29} and *n*-C_{31} (−28.4 ± 2.7‰ and −28.4 ± 2.4‰, respectively). Hence, it is most likely that the thermally matured petroleum-derived OC is being contributed to the sedimentary OC pool in the eastern Yellow Sea, albeit a much smaller amount than that of terrestrial-derived OC. Accordingly, our study demonstrates that molecular distributions and compound-specific $\delta^{13}C$ values of *n*-alkanes provide a useful approach for better understanding sources of sedimentary OC in the eastern Yellow Sea. Our approach also shows a great potential for the assessment of $\delta^{13}C$ of *n*-alkanes for the representative molecular pattern classified by the PCA and subsequent HCPC analyses. Future works should include the investigation of marine and terrestrial plants, suspended particulate matter in rivers, and organic aerosols to constrain the end-member values of each natural and anthropogenic source for the calculation of their relative contributions.

Acknowledgements

We thank J.-K. Gal and S. Kang for their analytical assistance in the laboratory at Hanyang University and the crew of the R/V Eardo for retrieving the cores. We also acknowledge Yoshito Chikaraishi

and two anonymous reviewers who contributed to the improvement of this manuscript with their suggestions. This research was a part of the project entitled "The Study of Marine Geology and Geological Structures in Korean Jurisdictional Seas" funded by the Korean Ministry of Oceans and Fisheries (PM58731). This work was also supported by the National Research Foundation of Korea grant funded by the Korea government (MSIP) (No. NRF-2016R1A2B3015388).

Appendix A. Supplementary data

Supplementary data related to this article can be found at http://dx.doi.org/10.1016/j.chemosphere.2016.11.110.

References

Alexander, C.R., DeMaster, D.J., Nittrouer, C.A., 1991. Sediment accumulation in a modern epicontinental-shelf setting: the Yellow Sea. Mar. Geol. 98, 51–72.
Baas, M., Pancost, R., van Geel, B., Sinninghe Damsté, J.S., 2000. A comparative study of lipids in Sphagnum species. Org. Geochem. 31, 535–541.
Ballentine, D.C., Macko, S.A., Turekian, V.C., Gilhooly, W.P., Martincigh, B., 1996. Compound specific isotope analysis of fatty acids and polycyclic aromatic hydrocarbons in aerosols: implications for biomass burning. Org. Geochem. 25, 97–104.
Barnes, M.A., Barnes, W.C., 1978. Organic compounds in lake sediments. In: Lerman, A. (Ed.), Lakes: Chemistry, Geology, Physics. Springer-Verlag, Berlin, pp. 127–152.
Berner, R.A., 1982. Burial of organic carbon and pyrite sulfur in the modern ocean – its geochemical and environmental significance. Am. J. Sci. 282, 451–473.
Bi, X., Sheng, G., Liu, X., Li, C., Fu, J., 2005. Molecular and carbon and hydrogen isotopic composition of n-alkanes in plant leaf waxes. Org. Geochem. 36, 1405–1417.
Bird, M.I., Summons, R.E., Gagan, M.K., Roksandic, Z., Dowling, L., Head, J., Fifield, L.K., Cresswell, R.G., Johnson, D.P., 1995. Terrestrial vegetation change inferred from n-alkane d13C analysis in the marine environment. Geochim. Cosmochim. Acta 59, 2853–2857.
Bourbonniere, R.A., Meyers, P.A., 1996. Sedimentary geolipid records of historical changes in the watersheds and productivities of Lakes Ontario and Erie. Limnol. Oceanogr. 41, 352–359.
Brassell, S.C., Eglinton, G., Maxwell, J.R., Philp, R.P., 1978. Natural background of alkanes in the aquatic environment. In: Hutzinger, O., van Lelyveld, I.H., Zoetman, B.C.J. (Eds.), Aquatic Pollutants: Transformation and Biological Effects. Pergamon Press, Oxford, pp. 69–86.
Brassell, S.C., Eglinton, G., 1980. Environmental chemistry – an interdisciplinary subject, Natural and pollutant organic compounds in contemporary aquatic environments. In: Albaiges, J. (Ed.), Analytical Techniques in Environmental Chemistry. Pergamon, Oxford.
Bray, E.E., Evans, E.D., 1961. Distribution of n-paraffins as a clue to recognition of source rocks. Geochim. Cosmochim. Acta 22, 2–15.
Canuel, E.A., Freeman, K.H., Wakeham, S.G., 1997. Isotopic composition of lipid biomarker compounds in estuarine plants and surface sediments. Limnol. Oceanogr. 42, 1570–1583.
Canuel, E.A., Martens, C.S., 1993. Seasonal variations in the sources and accumulation of organic matter associated with recently-deposited sediments. Org. Geochem. 20, 563–577.
Chen, C.T.A., Borges, A.V., 2009. Reconciling opposing views on carbon cycling in the coastal ocean: continental shelves as sinks and near-shore ecosystems as sources of atmospheric CO_2. Deep Sea Res. Part II 56, 578–590.
Chikaraishi, Y., Naraoka, H., 2003. Compound-specific δD–δ^{13}C analyses of *n*-alkanes extracted from terrestrial and aquatic plants. Phytochemistry 63, 361–371.
Collister, J.W., Rieley, G., Stern, B., Eglinton, G., Fry, B., 1994. Compound-specific δ^{13}C analyses of leaf lipids from plants with differing carbon dioxide metabolisms. Org. Geochem. 21, 619–627.
Collister, J.W., Summons, R.E., Lichtfouse, E., Hayes, J.M., 1992. An isotopic biogeochemical study of the Green River oil shale. Org. Geochem. 19, 265–276.
Cranwell, P.A., 1973. Chain-length distribution of *n*-alkanes from lake sediments in relation to post-glacial environmental change. Freshw. Biol. 3, 259–265.
Cranwell, P.A., 1984. Lipid geochemistry of sediments from Upton Broad, a small productive lake. Org. Geochem. 7, 25–37.
Cranwell, P.A., Eglinton, G., Robinson, N., 1987. Lipids of aquatic organisms as potential contributors to lacustrine sediments–II. Org. Geochem. 11, 513–527.
Eglinton, G., Hamilton, R.J., 1967. Leaf epicuticular waxes. Science 156, 1322–1335.
Ficken, K.J., Li, B., Swain, D.L., Eglinton, G., 2000. An *n*-alkane proxy for the sedimentary input of submerged/floating freshwater aquatic macrophytes. Org. Geochem. 31, 745–749.
Freeman, K.H., Hayes, J.M., Trendel, J.M., Albrecht, P., 1990. Evidence from carbon isotope measurements for diverse origins of sedimentary hydrocarbons. Nature 343, 254–256.
Garcin, Y., Schwab, V.F., Gleixner, G., Kahmen, A., Todou, G., Séné, O., Onana, J.-M., Achoundong, G., Sachse, D., 2012. Hydrogen isotope ratios of lacustrine sedimentary *n*-alkanes as proxies of tropical African hydrology: insights from a calibration transect across Cameroon. Geochim. Cosmochim. Acta 79, 106–126.
Gough, M.A., Rowland, S.J., 1990. Characterization of unresolved complex mixture of hydrocarbons in petroleum. Nature 344, 648–650.
Grimalt, J., Albaiges, J., 1987. Sources and occurrence of C_{12}–C_{22} *n*-alkane distributions with even carbon-number preference in sedimentary environments. Geochim. Cosmochim. Acta 51, 1379–1384.
Han, J., Calvin, M., 1969. Hydrocarbon distribution of algae and bacteria, and microbiological activity in sediments. Proc. Natl. Acad. Sci. (USA) 64, 436–443.
Han, J., McCarthy, E.D., Van Hoeven, W., Calvin, M., Bradley, W.H., 1968. Organic geochemical studies, II. A preliminary report on the distribution of aliphatic hydrocarbons in algae, in bacteria, and in a recent lake sediment. Proc. Natl. Acad. Sci. (USA) 59, 29–33.
Hayes, J.M., 1993. Factors controlling ^{13}C contents of sedimentary organic compounds: principles and evidence. Mar. Geol. 113, 111–125.
Hedges, J.I., Keil, R.G., Benner, R., 1997. What happens to terrestrial organic matter in the ocean? Org. Geochem. 27, 195–212.
Hu, L., Guo, Z., Feng, J., Yang, Z., Fang, M., 2009. Distributions and sources of bulk organic matter and aliphatic hydrocarbons in surface sediments of the Bohai Sea, China. Mar. Chem. 113, 197–211.
Huang, Y., Street-Perrott, F.A., Perrott, R.A., Metzger, P., Eglinton, G., 1999. Glacial-interglacial environmental changes inferred from molecular and compound-specific δ^{13}C analyses of sediments from Sacred Lake. Mt. Kenya. Geochim. Cosmochim. Acta 63, 1383–1404.
Jaffé, R., Mead, R., Hernandez, M.E., Peralba, M., DiGuida, O.A., 2001. Origin and transport of sedimentary organic matter in two subtropical estuaries: a comparative, biomarker-based study. Org. Geochem. 32, 507–526.
Jeng, W.L., Huh, C.A., 2004. Lipids in suspended matter and sediments from the East China Sea Shelf. Org. Geochem. 35, 647–660.
Kristen, I., Wilkes, H., Vieth, A., Zink, K.G., Plessen, B., Thorpe, J., Partridge, T.C., Oberhansli, H., 2010. Biomarker and stable carbon isotope analyses of sedimentary organic matter from Lake Tswaing: evidence for deglacial wetness and early Holocene drought from South Africa. J. Paleolimnol. 44, 143–160.
Mazurek, M.A., Simoneit, B.R.T., 1984. Characterization of biogenic and petroleum-derived organic matter in aerosols over remote, rural and urban areas. In: Keith, L.H. (Ed.), Identification and Analysis of Organic Pollutants in Air. Ann Arbor Science/Butterworth, Boston, pp. 353–370.
Mead, R., Xu, Y., Chong, J., Jaffé, R., 2005. Sediment and soil organic matter source assessment as revealed by the molecular distribution and carbon isotopic composition of *n*-alkanes. Org. Geochem. 36, 363–370.
Meyers, P.A., Ishlwatari, R., 1993. The early diagenesis of organic matter in lacustrine sediments. In: Engel, M., Macko, S.A. (Eds.), Organic Geochemistry. Plenum, New York, pp. 185–209.
Mille, G., Asia, L., Guiliano, M., Malleret, L., Doumenq, P., 2007. Hydrocarbons in coastal sediments from the Mediterranean Sea (Gulf of Fos area, France). Mar. Pollut. Bull. 54, 566–575.
Milliman, J.D., Syvitski, J.P., 1992. Geomorphic/tectonic control of sediment discharge to the ocean: the importance of small mountainous rivers. J. Geol. 525–544.
Ogura, K., Machihara, T., Takada, H., 1990. Diagenesis of biomarkers in Biwa lake sediments over 1 million years. Org. Geochem. 16, 805–813.
Pedentchouk, N., Sumner, W., Tipple, B., Pagani, M., 2008. δ^{13}C and δD compositions of *n*-alkanes from modern angiosperms and conifers: an experimental set up in central Washington State, USA. Org. Geochem. 39, 1066–1071.
Poynter, J.G., Eglinton, G., 1990. The molecular composition of three sediments from Hole 717C, the Bengal Fan. In: Cochran, J.R., Stow, D.A.V. (Eds.), Procedures of the Ocean Drilling Program Scientific Results Section, 116, pp. 155–161.
Prahl, F.G., Ertel, J.R., Goñi, M.A., Sparrow, M.A., Eversmeyer, B., 1994. Terrestrial organic carbon contributions to sediments on the Washington margin. Geochim. Cosmochim. Acta 58, 3035–3048.
R Development Core Team, 2015. R: a Language and Environment for Statistical Computing. R Foundation for Statistical Computing, Vienna, Austria. http://www.R-project.org.
Rommerskirchen, F., Plader, A., Eglinton, G., Chikaraishi, Y., Rullkötter, J., 2006. Chemotaxonomic significance of distribution and stable isotopic composition of long-chain alkanes and alkan-1-ols in C_4 grass waxes. Org. Geochem. 37, 1303–1332.
Scarlett, A., Galloway, T.S., Rowland, S.J., 2007. Chronic toxicity of unresolved complex mixtures (UCM) of hydrocarbons in marine sediments. J. Soils Sediments 7, 200–206.
Schouten, S., Klein Breteler, W.C.M., Blokker, P., Schogt, N., Rijpstra, W.I.C., Grice, K., Baas, M., Sinninghe Damsté, J.S., 1998. Biosynthetic effects on the stable carbon isotopic compositions of algal lipids: implications for deciphering the carbon isotopic biomarker record. Geochim. Cosmochim. Acta 62, 1397–1406.
Sikes, E.L., Uhle, M.E., Nodder, S.D., Howard, M.E., 2009. Sources of organic matter in a coastal marine environment: Evidence from *n*-alkanes and their δ^{13}C distributions in the Hauraki Gulf, New Zealand. Mar. Chem. 113, 149–163.
Simoneit, B.R.T., 1984. Organic matter of the troposphere: III. Characterization and sources of petroleum and pyrogenic residues in aerosols over the western United States. Atmos. Environ. 18, 51–67.
Simoneit, B.R.T., Chester, R., Eglinton, G., 1977. Biogenic lipids in particulates from the lower atmosphere over the eastern Atlantic. Nature 267, 682–685.
Smith, E., Wraige, E., Donkin, P., Rowland, S., 2001. Hydrocarbon humps in the marine environment: synthesis, toxicity, and aqueous solubility of

monoaromatic compounds. Environ. Toxicol. Chem. 20, 2428–2432.
Tao, S., Eglinton, T.I., Montluçon, D.B., McIntyre, C., Zhao, M., 2015. Pre-aged soil organic carbon as a major component of the Yellow River suspended load: regional significance and global relevance. Earth Planet. Sci. Lett. 414, 77–86.
Tissot, B., Pelet, R., Roucache, J., Combaz, A., 1977. Alkanes as geochemical fossils-indicators of geological environments. In: Campos, R., Goñi, J. (Eds.), Advances in Organic Geochemistry 1975. Enadimsa, Madrid, pp. 117–154.
van der Meer, M.T.J., Schouten, S., de Leeuw, J.W., Ward, D.M., 2000. Autotrophy of green non-sulphur bacteria in hot spring microbial mats: biological explanations for isotopically heavy organic carbon in the geological record. Environ. Microbiol. 2, 428–435.
Viso, A.-C., Pesando, D., Bernard, P., Marty, J.-C., 1993. Lipid components of the Mediterranean seagrass Posidonia Oceanica. Phytochemistry 34, 381–387.
Wang, Z., Fingas, M., Page, D.S., 1999. Oil spill identification. J. Chromatogr. A 843, 369–411.
Wiesenberg, G.L.B., Schwarzbauer, J., Schmidt, M.W.I., Schwark, L., 2004. Source and turnover of organic matter in agricultural soils derived from n-alkane/n-carboxylic acid compositions and C-isotope signatures. Org. Geochem. 35, 1371–1393.
Xing, L., Tao, S., Zhang, H., Liu, Y., Yu, Z., Zhao, M., 2011. Distributions and origins of lipid biomarkers in surface sediments from the southern Yellow Sea. Appl. Geochem. 26, 1584–1593.
Xing, L., Zhao, M., Gao, W., Wanga, F., Zhang, H., Li, L., Liu, J., Liu, Y., 2014. Multiple proxy estimates of source and spatial variation in organic matter in surface sediments from the southern Yellow Sea. Org. Geochem. 76, 72–81.
Yang, S., Jung, H.S., Lim, D.I., Li, C.X., 2003. A review on the provenance discrimination of sediments in the Yellow Sea. Earth Sci. Rev. 63, 93–120.
Yang, S., Youn, J.-S., 2007. Geochemical compositions and provenance discrimination of the central south Yellow Sea sediments. Mar. Geol. 243, 229–241.
Yoon, S.-H., Kim, J.-H., Yi, H.-I., Yamamoto, M., Gal, J.-K., Kang, S., Shin, K.-H., 2016. Source, composition and reactivity of sedimentary organic carbon in the river-dominated marginal seas: a study of the eastern Yellow Sea (the northwestern Pacific). Cont. Shelf Res. 125, 114–126.